Physics of Fluids ARTICLE scitation.org/journal/phf

Capillary breakup and extensional rheology response of food thickener cellulose gum (NaCMC) in salt-free and excess salt solutions

Cite as: Phys. Fluids 32, 012113 (2020); doi: 10.1063/1.5128254
Submitted: 18 September 2019 • Accepted: 8 January 2020 •
Published Online: 27 January 2020

View Online Export Citation CrossMark

Leidy Nallely Jimenez, Carina D. V. Martínez Narváez, and Vivek Sharma[a]

AFFILIATIONS

Department of Chemical Engineering, University of Illinois at Chicago, Chicago, Illinois 60607, USA

Note: This paper is part of the Special Topic on Food and Fluids.
[a]**Author to whom correspondence should be addressed:** viveks@uic.edu

ABSTRACT

Cellulose gum, also known as sodium carboxymethyl cellulose (NaCMC), is a polysaccharide often used as a thickener or rheology modifier in many industrial complex fluids, including foods. Shear and extensional rheology response influence production and processing of food, as well as the consumer perception and bioprocessing that begin with every bite. Stream-wise velocity gradients associated with extensional flows spontaneously arise during extrusion, calendaring, coating, dispensing, bubble growth or collapse, as well as during consumption including swallowing and suction via straws. The influence of polysaccharides on shear rheology response is fairly well characterized and utilized in food industry. In contrast, elucidating, measuring, and harnessing the extensional rheology response have remained longstanding challenges and motivate this study. The characterization challenges include the lack of robust, reliable, and affordable methods for measuring extensional rheology response. The product design challenges stem from the difficulties in assessing or predicting the influence of macromolecular properties on macroscopic rheological behavior. In this contribution, we address the characterization challenges using dripping-onto-substrate (DoS) rheometry protocols that rely on analysis of capillary-driven thinning and breakup of liquid necks created by releasing a finite volume of fluid onto a substrate. The DoS rheometry protocols emulate the heuristic tests of thickening, stickiness, or cohesiveness based on dripping a sauce from a ladle. We show that adding glycerol or changing salt concentration can be used for tuning the pinch-off dynamics, extensional rheology response, and processability of unentangled solutions of cellulose gum, whereas entangled solutions are relatively insensitive to changes in salt concentration.

Published under license by AIP Publishing. https://doi.org/10.1063/1.5128254

INTRODUCTION

Polysaccharides are widely used as rheology modifiers[1–6] in consumer products, including food,[1–4] inks, paints and coatings,[7] pharmaceuticals,[8] and cosmetics.[9] In biological systems, polysaccharides influence stickiness or stringiness of synovial fluids,[10,11] mucus,[12] and the deadly viscoelastic fluids found in carnivorous plants.[13,14] The addition of a relatively small concentration (<1% by weight) of polysaccharides such as cellulose gum, guar gum, and xanthan gum often leads to a substantial increase in zero shear viscosity and to highly shear thinning behavior for formulations.[15–23] As foods are multicomponent soft materials that often contain dispersed drops, bubbles, particles, or proteins,[24,25] an enhanced shear viscosity at low rates increases dispersion stability and homogeneity.[2,3,15–26] A decrease in shear viscosity at intermediate rates ($10^0 \leq \dot{\gamma} \leq 10^2\,s^{-1}$) facilitates pouring and mixing, and a further decrease at higher rates facilitates processing operations such as extrusion, coating, spraying, and dispensing.[4,7] Even when polysaccharides are added to aid in retention of water and flavors, formation of film or fibers, manage calorie count, or provide texture in gluten-free or low-fat products,[16,21,27,28] they still alter rheology or perceived runniness, cohesiveness, and mouth-feel.[16,29,30] Product and process design for food is often based on measured shear rheology response.[2,3,15–31] However, stream-wise velocity gradients associated with extensional flows spontaneously arise in converging channels or thinning liquid necks and films in many operations

Published under license by AIP Publishing

related to foods[3,26] including dispensing, spraying, dip-coating, dripping, printing, growth of bubbles or drops, extrusion, and spreading, as shown schematically in Fig. 1. For polymeric complex fluids, the resistance to stretching flows defined as extensional viscosity, η_E, cannot be estimated or computed from measurement of shear rheology response.[32–35] Even though extensional rheology response plays a critical role in determining the production, processing, consumption, and sensory perception of foods,[3,30,36–43] two significant challenges exist that motivate this study: (a) a reliable, repeatable measurement with deformation history or flow rates that emulate extensional flows encountered in culinary applications and (b) an understanding of the connection between macroscopic rheological measures and macromolecular hydrodynamics and thermodynamics.

Unlike Newtonian fluids that exhibit a constant Trouton ratio, $Tr = \eta_E/\eta = 3$, polymer solutions can display relatively high values and $Tr > 10^2$ are routinely observed.[33–35] Furthermore, many shear thinning polymeric fluids show dramatic strain hardening in response to strong extensional flows.[33–35] Even though shear rheology measurements are fairly routine and standardized, the extensional rheology characterization relies on bespoke experimental protocols[32–35,48] and reveal markedly different response in different techniques, showing high sensitivity to both strain and strain rate, and entire deformation history. In the context of food applications, the challenges are optimally expressed in this quote from Fischer and Windhab:[3] "*Approaches that aim to introduce extensional rheometry are extremely useful to understand the material but are complicated by the fact that measuring devices are expensive, do not operate in the production time scale, and do not provide instrumental readings easily be transferred to the process or to the baker at four o'clock in the morning.*" In this contribution, we demonstrate that the dripping-onto-substrate (DoS) rheometry protocols[49–53] (that

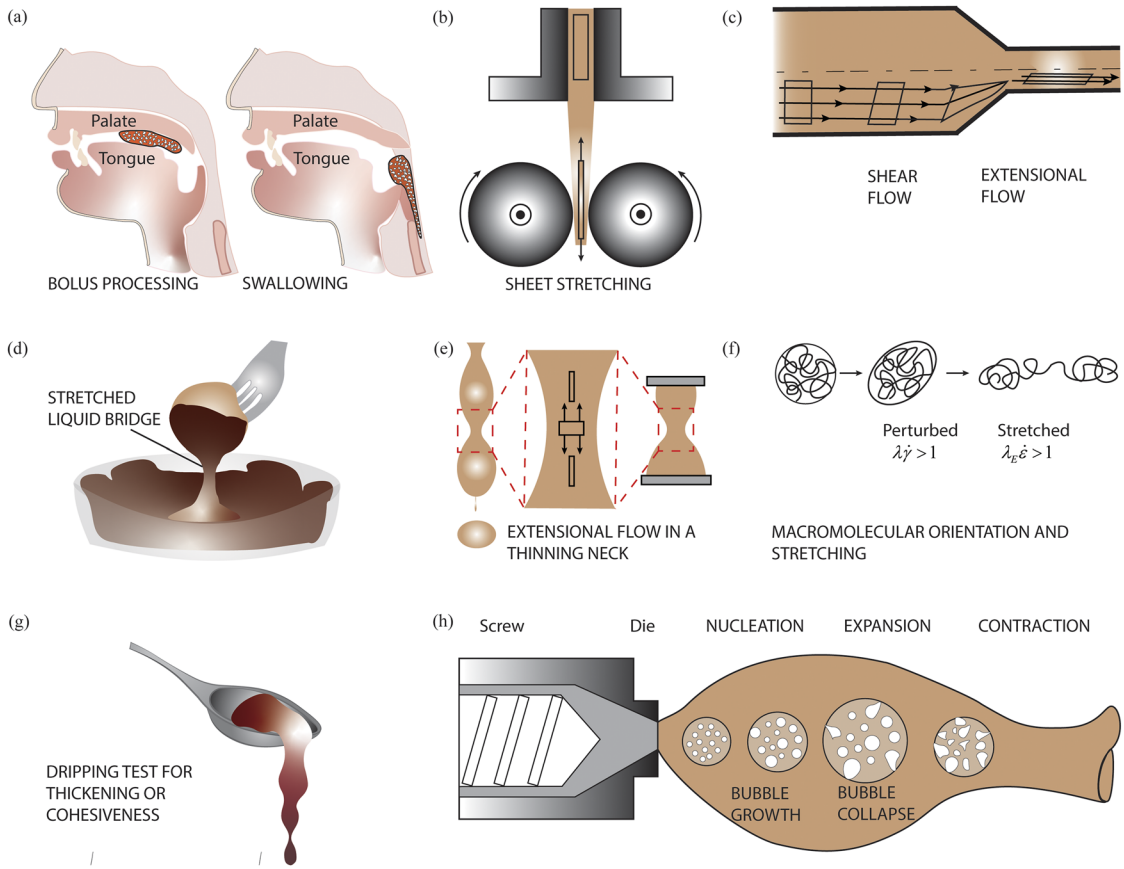

FIG. 1. Extensional flows in gastronomy and food engineering. (a) Consumption of food involves both shear and extensional flows, and thickeners are often added to design food with suitable mouth-feel and texture[38] and to aid dysphagia patients in swallowing.[30,38–40] (b) Sheet stretching, showing deformation of a control volume. (c) Converging channels in extrusion are associated with extensional flows, though shear flows also arise near the wall. (d) In dipping sauces, the time to breakup and the breakup length of the liquid bridge are product design considerations. (e) Capillary-driven thinning of necks creates stream-wise velocity gradients associated with extensional flows. (f) Macromolecular conformational changes in the presence of shear and extensional flows. In contrast to shear flows that weakly perturb macromolecular coils, strong extensional flow fields can unravel the chains, leading to a pronounced coil-stretch transition for flexible neutral polymers.[44–47] (g) Dripping sauce or chocolate, or kitchen experiments aimed at checking thickening of a soup. (h) Strain hardening, contributed by gluten or polysaccharides (used as gluten alternatives), determines bubble growth and collapse and ultimately sets texture and mouth-feel.[41–43]

Published under license by AIP Publishing

we developed recently) can address such characterization challenges. The DoS rheometry protocols involve the visualization and analysis of capillary-driven thinning and breakup of a self-thinning liquid neck generated in an unstable liquid bridge formed by releasing a finite volume of fluid from a nozzle onto a partially wetting substrate. The extensional rheology characterization for high viscosity complex fluids can be often carried out economically, reliably, and repeatedly by using off-the-shelf digital cameras for capturing neck shape and shape evolution.[51,54]

The capillary-driven thinning and pinch-off dynamics of simple, Newtonian fluids are dictated by the interplay of inertial, viscous, and capillary stresses.[33,55–57] Additional viscoelastic stresses associated with stretching, relaxation, and orientation of macromolecules [see Fig. 1(f)] in response to extensional flows in thinning necks often result in a measurable delay in thinning and pinch-off.[49–53,58–66] Analysis of neck thinning dynamics for measurement of transient, $\eta_E = \eta_E(\dot{\varepsilon}, \varepsilon, t)$, as well as steady terminal extensional viscosity, η_E^{∞}, and extensional relaxation time, λ_E, is the basis for DoS rheometry as well as techniques that create a stretched liquid bridge by applying a step strain to the fluid confined between two parallel plates.[33,58–64] However, as the commercially available technique called CaBER (capillary breakup extensional rheometer)[33,63,64] relies on step strain that requires nearly 50 ms, pinch-off occurs before plate separation for low viscosity (η < 50 mPa s), low elasticity (relaxation time, λ < 1 ms) fluids. Therefore, the countable few published studies that utilize CaBER (or devices based on step strain) focus on relatively high molecular weight polysaccharides (typically $M_w > 10^6$ Da) at relatively high concentrations (>0.5 wt. %).[18,19,61,62,67–74] Campo-Deano and Clasen[75] showed that modifying the CaBER protocol by using the slow retraction method (SRM) allows access to lower relaxation times than accessible with typical CaBER measurements. However, as SRM requires staged stretching of the liquid bridge,[75] the deformation history fails to emulate real dispensing flows and the filament lifespan (breakup time) is not measured. Additionally, the capillary thinning and pinch-off dynamics of structured complex fluids, including polysaccharide gels formed at higher concentrations, are sensitive to the rate and extent of the initial step strain in all CaBER measurements.[73,75–77] Although we have established that the DoS rheometry protocols can be used for characterizing the extensional rheology response for solutions of both neutral and charged polymers,[49–51] well below the sensitivity range of CaBER, the characterization challenges for charged polysaccharide solutions have not been tackled so far.

In the present contribution, we carry out a systematic investigation of the rheological response of solutions of a relatively low molecular weight (M_w = 250 kDa) polysaccharide called cellulose gum or sodium carboxymethyl cellulose (NaCMC). Cellulose gum is used quite extensively as a rheology modifier (thickener, gelator, stabilizer, or texture enhancer) in food products such as ice creams, juices, jellies, soups, beer, as well as in dairy, bakery, and meat products.[15,17,20–23] In many applications, NaCMC is added in the presence of salt, and often glycerol labeled as additive E422 is added for influencing viscosity (of liqueurs, for example), hygroscopic nature, sweetness, calorie count, solvent quality, and the perceived texture and mouth-feel.[78] The addition of glycerol changes solvent viscosity, dielectric constant (electrostatic interactions), density, surface tension (free surface flows), refractive index, and solvent quality (coil size and excluded volume interactions). Unlike most of the published studies that focus on shear rheology characterization of aqueous NaCMC solutions,[15,17,20–23,29,31,67,79–89] in this contribution, we characterize the influence of both added glycerol and added salt on both shear and extensional rheology response and investigate capillary breakup and dispensing behavior of these food thickener solutions.

MATERIALS AND METHODS

Cellulose gum or sodium carboxymethyl cellulose (NaCMC) solutions

Sodium carboxymethyl cellulose of M_w = 250 kDa was purchased from Sigma-Aldrich, with the degree of substitution (DS) specified by the manufacturer to be 0.8–0.95 and was used without further purification. Aqueous polyelectrolyte solutions were prepared first, by slowly and carefully adding dry polymer powder to deionized water. The aqueous polymer solutions were left on a roller for a minimum of three days to ensure slow and complete mixing without chain breakup that is usually associated with high mixing flows. Glycerol and salt were added after the cellulose gums dissolved in water, and the solutions were left on a roller for four extra days on glycerol addition and for additional 2–3 days on subsequent salt addition.

Shear rheology characterization

The shear rheology response of sodium carboxymethyl cellulose (NaCMC) solutions was characterized using a concentric cylinder (double gap) Couette cell and cone and plate geometry (cone diameter of 50 mm and cone angle of 1°) on an Anton Paar MCR 302 rheometer at 25 °C. For typical measurements, the shear rate in the range of 1–10^3 s^{-1} was applied to the polyelectrolyte solutions to measure shear stress and determine the steady shear viscosity, $\eta(\dot{\gamma}) = \tau/\dot{\gamma}$.

Extensional rheology characterization using dripping-onto-substrate (DoS) rheometry

The experimental system used for DoS rheometry consists of a dispensing system and an imaging system, shown in Fig. 2. A finite volume of fluid is dispensed through a stainless steel nozzle onto a clean glass substrate at a height H below the nozzle. The radius of the nozzle is kept constant for all experiments, with an outer diameter of $D_0 = 2R_0$ = 1.27 mm and inner diameter of D_i = 0.838 mm. The flow rate was fixed, Q = 0.02 ml/min, and an aspect ratio of $H/D_0 \approx 3$ was used. The imaging system includes a light source, diffuser, and high speed camera (Fastcam SA3). A Nikkor 3.1× zoom (18–25 mm) lens is also used with a macro lens to maximize magnification at the frame rates used (8000–25 000 fps). The DoS videos are further analyzed with ImageJ and specially written MATLAB codes for determination of the minimum neck radius from every snapshot. Several recent publications provide details about DoS rheometry protocols and describe pinch-off dynamics and extensional rheology response for complex fluids, ranging from polymer and polyelectrolyte solutions[49–54,90–93] to inks[51,94] to micellar solutions,[51,95–97] as well as multicomponent power law fluids.[51]

Published under license by AIP Publishing

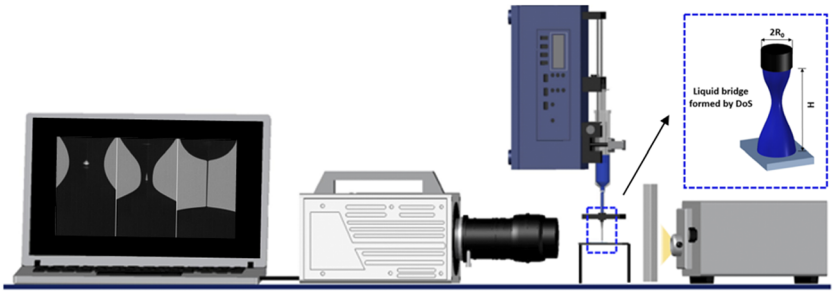

FIG. 2. Schematic for Dripping-onto-Substrate (DoS) rheometry. A liquid bridge with neck that undergoes thinning is formed by dispensing a desired amount of test fluid through a nozzle placed at a height *H* above a glass substrate. A light source with a diffuser is utilized for backlighting the liquid bridge, and the images are captured using a high speed camera (equipped with suitable magnification optics) connected to a laptop used for image acquisition and subsequently for image analysis.

RESULTS AND DISCUSSION

Steady shear viscosity of NaCMC solutions: Influence of glycerol and salt

Steady shear viscosity of aqueous NaCMC solutions as a function of shear rate included in Figs. 3(a) and 3(b) shows the expected concentration-dependent increase in shear viscosity. Although a similar increase occurs for NaCMC solutions formulated in a glycerol-water mixture (70/30 w/w), a higher degree of shear thinning is exhibited in the mixed solvent (that itself has a higher viscosity of η_s = 0.018 Pa s). The zero shear viscosity, η_0, values, extracted from the rate-independent steady shear viscosity, are shown in Fig. 3(c). The exponent α obtained from power law fit ($\eta_0 \propto c^{\alpha}$) to the data (shown as solid lines) changes from α = 0.5 to 1.5 for aqueous and from α = 0.76 to 2.8 in the glycerol-water mixture (fits and errors are summarized in the supplementary material). The contribution of polymer to solution viscosity can be quantified by computing specific viscosity, $\eta_{sp} = (\eta_0 - \eta_s)/\eta_s$. As NaCMC is used as a thickener, we primarily focus on the rheological response for concentrations that give $\eta_{sp} > 1$ or lie in the non-dilute regime. Polymer solutions are considered dilute, with non-interacting coils, for concentrations below an overlap concentration, c^*, that can be defined as the concentration at which the volume available per polymer coil approaches pervaded volume of a coil, leading to solution viscosity twice that of pure solvent or η_{sp} = 1. We estimate the overlap concentration c^* = 0.007 wt. % for aqueous solutions and a much higher value c^* = 0.03 wt. % for solutions in the glycerol-water mixture, from the viscosity data shown in Fig. 3(d) by extrapolating to concentration where specific viscosity equals 1.

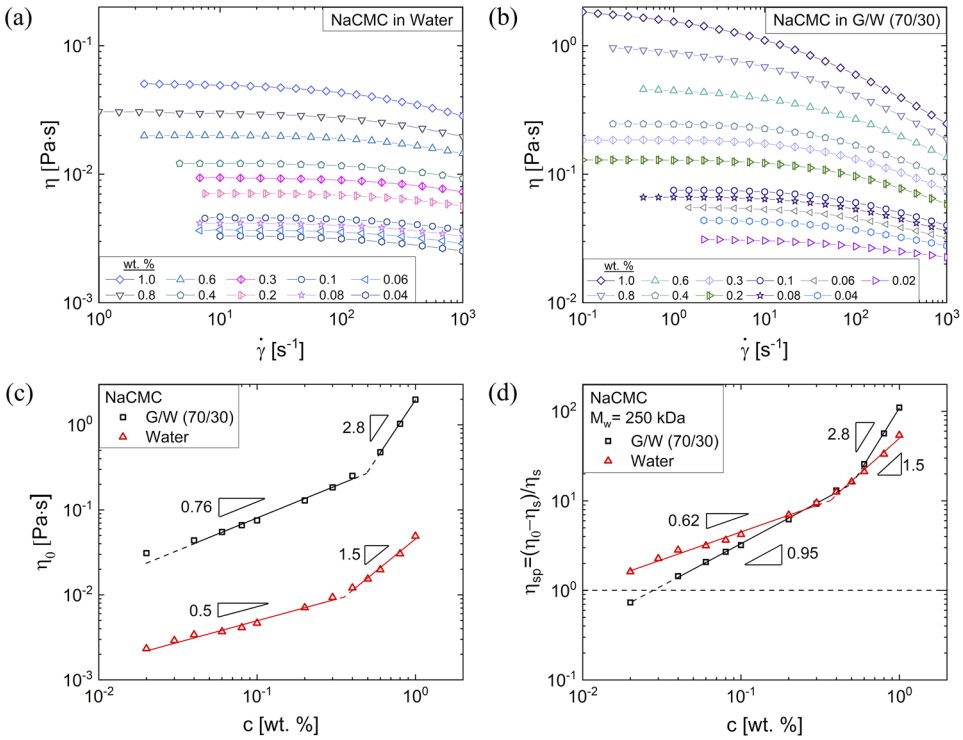

FIG. 3. Steady shear rheology response of NaCMC solutions in water contrasted with solutions in a glycerol-water mixture (70/30 w/w). (a) Steady shear viscosity as a function of shear rate for aqueous solutions exhibits a concentration-dependent increase and a slight shear thinning behavior at higher concentrations. (b) Steady shear viscosity as a function of shear rate of NaCMC in glycerol-water mixtures increases with concentration; however, the overall increase is higher compared to the aqueous case. (c) Concentration-dependent variation in zero shear viscosity appears to be stronger for the glycerol-water mixture. (d) Specific viscosity as a function of concentration: aqueous solutions exhibit scaling quite consistent with theoretical models and experiments described in the literature. Addition of glycerol decreases coil size in unentangled solutions, increases the background solvent viscosity, and also leads to a stronger concentration-dependent increase in viscosity values in both unentangled and entangled solutions.

Published under license by AIP Publishing

The intrinsic viscosity values estimated using $c^*[\eta] = 1$ are $[\eta]_W^{NaCMC} \approx 143$ dl/g and $[\eta]_{GW}^{NaCMC} \approx 33$ dl/g, respectively, which are comparatively large in contrast to $[\eta]^{PEO} \approx 6$ dl/g measured for aqueous polyethylene oxide (PEO) solution (neutral polymer in a good solvent, with $M_w = 1000$ kDa) or compared to $[\eta]^{EHEC} \approx 3.33$ dl/g measured for non-ionic ethyl hydroxyethyl cellulose (EHEC) with comparable $M_w = 240$ kDa.[49,98] The higher intrinsic viscosity values of aqueous solutions NaCMC compared to aqueous PEO or EHEC solutions are due to larger pervaded volume of the electrostatically stretched chains. The intrinsic viscosity values measured here for NaCMC decrease by 4.5 times in glycerol/water (70/30 w/w) mixtures, implying that the pervaded volume is much smaller. The overlap concentration and intrinsic viscosity values determined from our experimental data compare well with the corresponding values obtained by Lopez *et al.*[79–81] for aqueous NaCMC solutions made with polymer with similar M_w and DS (and possibly, similar amount of residual salt, for these were obtained from the same supplier). However, Lopez *et al.*[79–81] also determined that viscosity values give much higher overlap concentration ($c^* = 0.007$ wt. %) than obtained using scattering ($c^* = 0.0003$ wt. %). The specific viscosity vs concentration data shown in Fig. 3(d) exhibit two regimes: $\eta_{sp} \propto c^{0.62}$ and $\eta_{sp} \propto c^{3/2}$ in aqueous NaCMC solutions that too compare well with the values reported by Lopez *et al.*[80,81] The scaling in the first regime is similar to the $\eta_{sp} \propto c^{1/2}$ scaling, also referred to as the Fuoss law,[99–105] and reported to be the characteristic behavior for semi-dilute, unentangled polyelectrolyte solutions.[99–117] The $\eta_{sp} \propto c^{3/2}$ scaling observed in the second regime matches the scaling theory prediction for entangled polyelectrolyte solutions made by Dobrynin, Colby, and Rubinstein,[99–101,106] and the exponent is weaker than the value $\eta_{sp} \propto c^{1.7}$ predicted by Muthukumar.[104,105,112]

In contrast with aqueous solutions, a stronger concentration dependence of $\eta_{sp} \propto c^{0.95}$ and $\eta_{sp} \propto c^{2.8}$ is observed for the NaCMC solutions in the glycerol-water mixture (70/30 w/w), as shown in Fig. 3(d). On close inspection of the data shown in Fig. 3(d), we find that even though the entanglement concentration $c_e = 0.37$ wt. % for aqueous solution is comparable to $c_e = 0.5$ wt. % for solutions in the glycerol-water mixture, due to an increase in overlap concentration, the semi-dilute, unentangled region shrinks, as $c_e/c^* = 53$ decreases to $c_e/c^* = 17$ on addition of glycerol. Similarly, a stronger exponent for a concentration-dependent increase in specific viscosity $\eta_{sp} \propto c^{\alpha}$ in glycerol-water solutions was reported in an earlier study for unentangled poly(acrylic acid) (PAA) solutions ($\alpha = 0.7$ rather than 1/2) and entangled NaPSS solutions (1.1 rather than 0.85).[52] Glycerol has three hydroxyl groups that promote its solubility in water and provide sites for hydrogen bonding, and the addition of glycerol decreases the dielectric constant by nearly 2/3, thus decreasing both the magnitude and screening length of electrostatic interactions. Thus, the observed change in scaling or concentration range of the semi-dilute, unentangled regime observed in Fig. 3(d) on addition of glycerol is primarily due to the influence of electrostatics, with additional influence from changes in effective solvent quality, hydrophobic effect, and hydrogen bonding.

Addition of salt modifies shear rheology of NaCMC solutions

The influence of ionic strength on the steady shear viscosity is illustrated by the comparisons shown in Fig. 4(a) for two NaCMC (0.06 wt. % and 0.6 wt. %) solutions. Addition of salt, even at a relatively low concentration (0.005M NaCl), results in a profound decrease in the zero shear viscosity, and additional reduction occurs in a high salt concentration of 0.1M. The relative decrease in the steady shear viscosity is more pronounced at the lower polymer concentration [see the data for 0.06 wt. % in Fig. 4(a)]. A similar decrease in the zero shear viscosity on salt addition has been reported before for aqueous NaCMC solutions.[79–81] The specific viscosity as a function of the concentration of NaCMC plotted in Fig. 4(b) shows two distinct scaling regimes for $c/c^* > 1$ with $\eta_{sp} \propto c^{0.95}$ and $\eta_{sp} \propto c^{2.8}$, respectively, for no added salt solutions and $\eta_{sp} \propto c^{1.6}$ and $\eta_{sp} \propto c^{2.8}$ for excess salt (0.1M).

Upon addition of salt, the coil size decreases significantly, leading to an increase in overlap concentration to $c^* = 0.06$ wt. % for

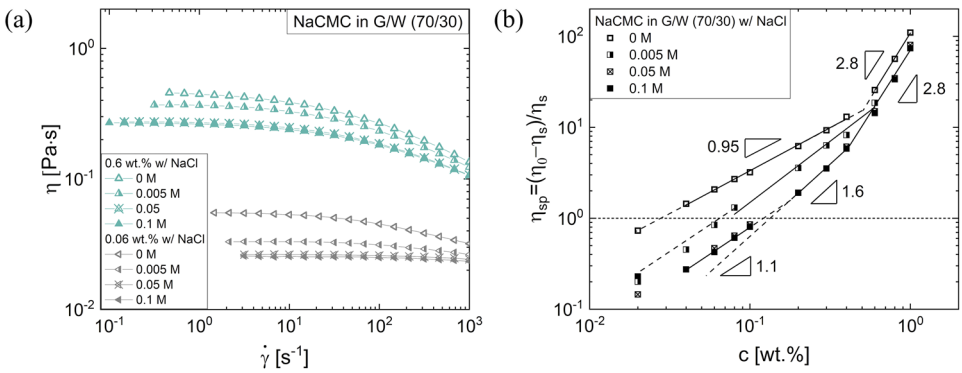

FIG. 4. Influence of added salt on shear viscosity of NaCMC solutions in the glycerol-water mixture (70/30 w/w). (a) Steady shear viscosity as a function of shear rate contrasting the effect of salt concentration for two polyelectrolyte concentrations: $c = 0.06$ wt. % and $c = 0.6$ wt. %. (b) Specific viscosity as a function of concentration shows two distinct scaling regimes for the salt-free case: $\eta_{sp} \propto c^{0.95}$ and $\eta_{sp} \propto c^{2.8}$ in the semi-dilute, unentangled and semi-dilute, entangled regimes, respectively. Even though the specific viscosity displays two distinct regimes for 0.05M and 0.1M NaCl that differ from the no added salt case, the $\eta_{sp} \propto c^{1.1}$ fit corresponds to the dilute regime, the $\eta_{sp} \propto c^{1.6}$ fit corresponds to the semi-dilute, unentangled regime, and the $\eta_{sp} \propto c^{2.8}$ fit corresponds to the semi-dilute, entangled regime.

Published under license by AIP Publishing

0.005M and c^* = 0.12 wt. % for 0.1M NaCl solutions, respectively, in comparison with c^* = 0.03 wt. % for solutions with no added salt prepared in the glycerol-water mixture (70/30 w/w). The corresponding intrinsic viscosity values are $[\eta]^{\text{NaCMC}}_{0.005\text{M}} \approx 16.5$ dl/g and $[\eta]^{\text{NaCMC}}_{0.1\text{M}} \approx 8.3$ dl/g. Since the specific viscosity values $\eta_{sp} < 1$ for c < 0.12% on addition of salt, in contrast to $\eta_{sp} < 1$ for $c < c^*$(=0.03 wt. %), the NaCMC in the glycerol-water mixture (no added salt) displays a semi-dilute regime over an extra decade of concentration. The semi-dilute, unentangled regime in excess salt (0.1M) exhibits $\eta_{sp} \propto c^{1.6}$ before transitioning to $\eta_{sp} \propto c^{2.8}$ in the semi-dilute, entangled regime. The specific viscosity values for NaCMC solutions in the glycerol-water mixture (70/30 w/w) without added salt and with excess salt (0.1M) exhibit similar magnitude and concentration dependence in the entangled regime.

Pinch-off dynamics of NaCMC solution in glycerol/water mixtures

Dripping-onto-substrate (DoS) rheometry protocols were utilized to visualize the capillary-driven thinning and breakup, and Figs. 5(a) and 5(b) show the image sequences obtained for unentangled NaCMC concentrations c = 0.02 wt. % and 0.06 wt. % in glycerol-water mixtures (70/30 w/w) with no added salt and 0.1M NaCl, respectively. Conical necks, connected to a sessile drop by a thin filament, appear in the image sequences shown in Figs. 5(a) and 5(b). The formation of a conical neck shape is a characteristic feature of the inertiocapillary (IC) thinning response exhibited during the capillary-driven thinning of low viscosity (inviscid) fluids such as water. The radius evolution data for IC response follows a viscosity-independent, power law expression[55,118–120] $R(t)/R_0 = X((t_f - t)/t_R)^{2/3}$, where R_0 is the outer radius of the nozzle, and the pre-factor X is historically quoted to have the value of either 0.8 or 0.65, although recent papers find a lower value of $X \approx 0.4$ for glycerol-water solutions.[121] Rayleigh time $t_R = (\rho R_0{}^3/\sigma)^{1/2}$ defines the characteristic time scale for inertiocapillary thinning[120–122] for a fluid with density, ρ, and surface tension, σ. In all three cases shown, a slender filament appears in the late stage and suggests a possible role for viscoelastic effects, contributed by stretching and orientation of macromolecular chains in response to strong uniaxial extensional flow encountered in the neck.

The overall pinch-off time, we hereafter refer to as filament lifespan, t_f, for NaCMC solutions in the glycerol-water mixture is less than 15 ms, whereas for aqueous NaCMC solutions, the filament lifespan is significantly shorter. Solutions with such low viscosities and short pinch-off times cannot be analyzed using CaBER measurements. The corresponding radius evolution plots for NaCMC solutions in the glycerol-water mixture (70/30 w/w) with salt-free and excess salt (0.1M NaCl) are included in Figs. 5(c) and 5(d) on a

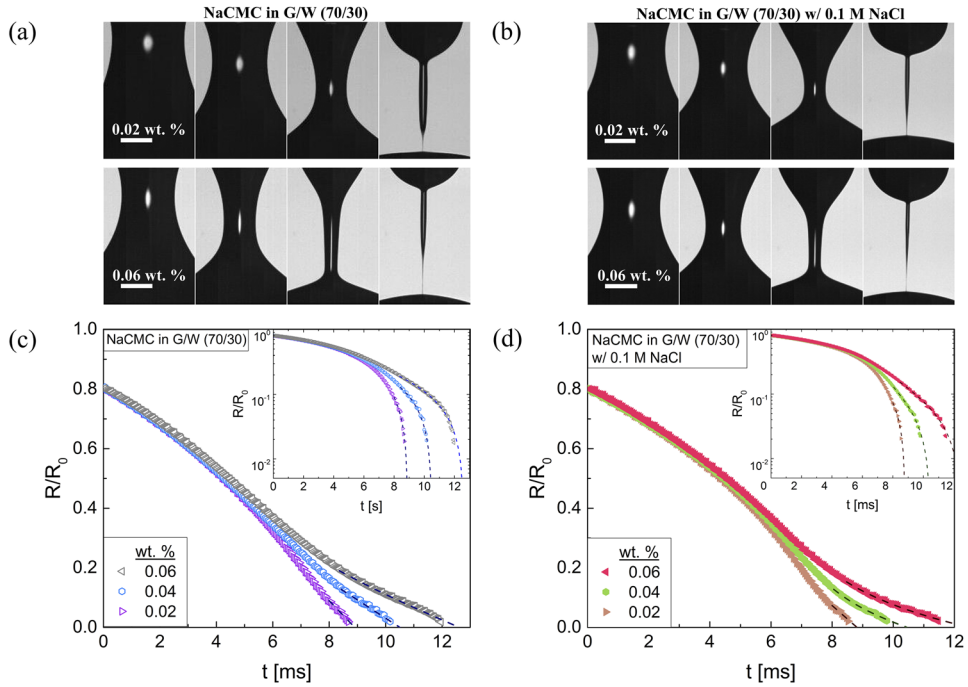

FIG. 5. Capillary thinning and breakup dynamics of NaCMC solutions in glycerol/water (70/30) mixtures. (a) Image sequences, acquired between 19 000–25 000 fps, for solutions with c = 0.02 wt. % and 0.06 wt. %, show that the thinning neck begins to assume conical shape, but a narrow cylindrical thread appears in the late stage. The conical shape is a characteristic feature of inertiocapillary thinning, and the appearance of the thread suggests that viscoelastic stresses are triggered before breakup. Images shown are 3 ms apart (supplementary material, videos). (b) Image sequences for the corresponding concentrations in a high salt system show that the addition of salt does not create a large change in the filament shape. The scale bar represents 0.5 mm. (c) Radius evolution data for solutions with salt-free is contrasted against (d) the datasets obtained for the solutions with excess salt (0.1M NaCl). The insets show the radius evolution plots on a semi-log scale, and the dotted lines show the fits used for extracting extensional viscosity and extensional relaxation time.

Published under license by AIP Publishing

linear-linear axis. Since radius evolution data for polymer solutions are typically plotted using log-linear plots, we included the semi-log version of radius evolution plots in the inset. The initial thinning dynamics is a solvent-driven, viscosity-independent inertiocapillary (IC) response, and hence, all the curves appear indistinguishable in the first stage. In the last stage leading to pinch-off, the radius evolution data show departure from the IC behavior, and as viscoelastic effects lead to concentration-dependent delay in pinch-off, the radius evolution data can be analyzed, as discussed next.

The Entov–Hinch model[123] or its variants discussed in Refs. 33, 61, 62, and 124–126 describe the neck thinning dynamics using three distinct regimes for polymer solutions in a viscous solvent: (I) initial inertiocapillary (IC) regime for low viscosity fluids or viscocapillary (VC) regime with a linear decrease in radius [Eq. (1)]; (II) intermediate elastocapillary (EC) regime, with an exponential decay in the neck radius [Eq. (2)]; and (III) a terminal visco-elastocapillary (TVEC) response [Eq. (3)] that arises due to finite extensibility effects. The three distinct scaling laws can be described by the following expressions:

$$\frac{R}{R_0} = 0.0709\left(\frac{t_{fv} - t}{t_{vc}}\right), \tag{1}$$

$$\frac{R(t)}{R_0} \approx \left(\frac{G_E R_0}{2\sigma}\right)^{1/3} \exp[-(t - t_c)/3\lambda_E], \tag{2}$$

$$\frac{R(t)}{R_0} = \frac{\sigma}{2R_0\eta_E^{\infty}}(t_f - t) = \frac{1/2}{Oh\,Tr^{\infty}}\left(\frac{t_f - t}{t_R}\right). \tag{3}$$

Here, t_{fv} represents the pinch-off time and the viscocapillary time $t_{vc} = \eta_0 R_0/\sigma$ represents a time scale for VC thinning set by the zero shear viscosity and surface tension. In the EC expression, the use of single exponential implies that elastocapillary thinning regime is dominated by a longest relaxation time, λ_E, and characterized by a constant Weissenberg number, $Wi_{EC} = \dot{\varepsilon}_{EC}\lambda_E = 2/3$. Expression (2) differs from the most often cited Entov–Hinch expression[123] in utilizing λ_E as a time scale different from the longest shear relaxation time, G_E, as an apparent extensional modulus and the computed elastocapillary behavior in terms of a shifted time scale, as detailed in our previous contributions.[49–53] Fitting the TVEC regime by Eq. (3) yields the measurements of steady, terminal extensional viscosity η_E^{∞}. Here, $Tr^{\infty} = \eta_E^{\infty}/\eta$ is the terminal Trouton ratio and t_f refers to the filament lifespan. For systems influenced by viscoelastic effects with short EC regimes and TVEC regimes present, the radius evolution can be fit using the following semi-empirical expression based on an equation proposed by Anna and McKinley:[63]

$$\frac{R(t)}{R_0} = A\exp(-B(t - t_c)) - C(t - t_c) + D. \tag{4}$$

Here, the parameter B can be interpreted as a measure of the longest relaxation time (approximately $B \approx 1/3\lambda_E$), while the parameter C can be used for determining the steady, terminal extensional viscosity value. The transition point, t_c, was obtained from the derivative dR/dt of the data, and filament lifespan can be determined from $t_f = t_c + (D/C)$. Image sequences, taken at 8000–19 000 fps, for concentrations $c = 0.4$ wt. %, $\Delta t = 10$ ms and 1 wt. %, $\Delta t = 40$ ms of no added salt and 0.1M NaCl solutions are shown in Figs. 6(a) and 6(b). In contrast to the conical neck shape observed for lower concentration solutions, as shown in Figs. 5(a) and 5(b), here the neck shape converges to a slender, cylindrical shape rather quickly. The radius evolution profiles are compared for four solutions each in the concentration range, $c = 0.4$–1 wt. %, that corresponds to semi-dilute,

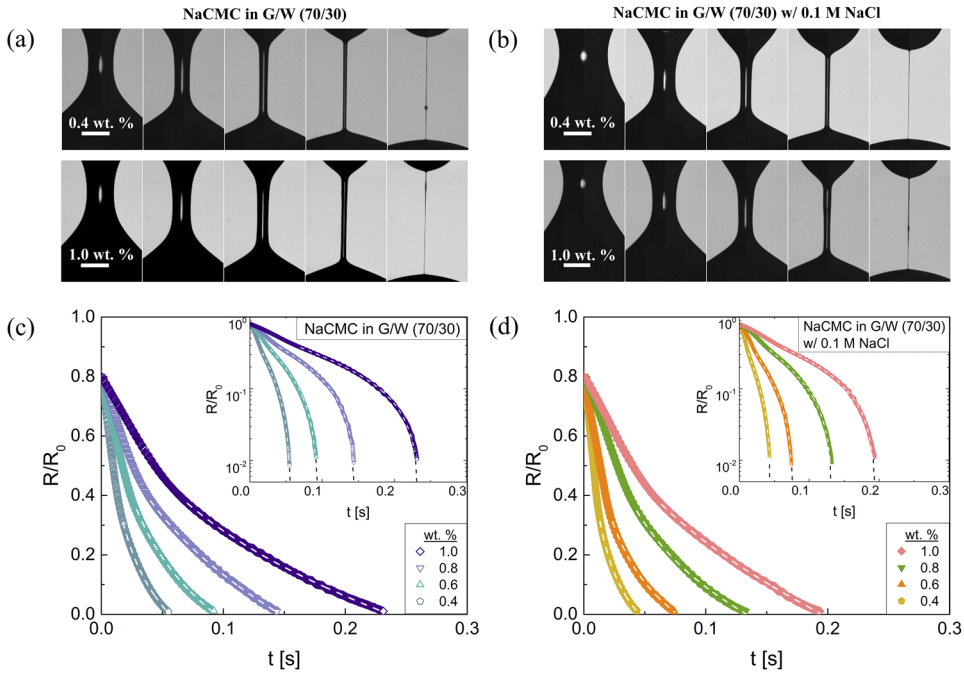

FIG. 6. Capillary thinning and pinch-off dynamics of NaCMC solutions in glycerol/water mixtures characterized using DoS rheometry. [(a) and (b)] Image sequences for $c = 0.4$ wt. % and $c = 1$ wt. % are contrasted for no salt and high salt (0.1M NaCl). The scale bar corresponds to 0.5 mm, and each frame is separated by 10 ms (supplementary material, videos). (c) Radius evolution data plotted on linear-linear axes for four concentrations in the range $c = 0.4$–1 wt. % (no added salt) show a concentration-dependent increase in filament lifespan. The corresponding data are also shown in the inset on semi-log axes. (d) Radius evolution data at matched concentrations for solutions with a high salt (0.1M NaCl).

Published under license by AIP Publishing

TABLE I. Concentration-dependent increase in measured values of zero shear viscosity obtained from steady shear viscosity data and corresponding values of extensional relaxation time, filament lifespan, and steady, terminal extensional viscosity obtained from the analysis of radius evolution data acquired using the DoS rheometry protocols.

NaCMC	No added salt				High salt (0.1M NaCl)			
c (wt. %)	η_0 (Pa·s)	λ_E (ms)	η_E^∞ (Pa·s)	t_f (ms)	η_0 (Pa·s)	λ_E (ms)	η_E^∞ (Pa·s)	t_f (ms)
0.04	0.044			11	0.023	0.39	1.1	10
0.06	0.055	0.7	1.2	13	0.026	0.66	1.7	12
0.08	0.066	0.84	1.6	15	0.029	0.81	2.0	12
0.1	0.075	1.3	2.0	16	0.032	1.0	2.4	13
0.2	0.13	2.9	5.7	29	0.052	2.2	6.2	20
0.3	0.18	4.3	7.2	40	0.081	2.8	7.1	28
0.4	0.25	5.4	9.8	50	0.12	4.2	9.2	40
0.6	0.48	9.4	14	85	0.27	7.4	14	68
0.8	1.0	16	18	135	0.62	13	19	119
1.0	2.0	27	28	228	1.3	21	24	183

entangled regimes for both no salt and high salt (0.1M NaCl) solutions. The values of extensional relaxation time, filament lifespan, and terminal extensional viscosity obtained after analyzing the data included in Figs. 5 and 6 are listed in Table I and discussed together with Figs. 8 and 9 later in the manuscript.

Transient extensional viscosity of entangled NaCMC solutions

The conformation changes that arise due to stretching and orientation from the extensional flow contribute to elastic stresses $\eta_E\dot{\varepsilon}$ that compete with the capillary stresses σ/R in the elastocapillary and finite extensibility (TVEC) regime. Using the value of radius as a function of time, the capillary or extensional stress as well as extension rate, $\dot{\varepsilon} = -2(dR/dt)/R$, can be computed and used for determining the apparent or transient extensional viscosity as follows:

$$\eta_E = \frac{\sigma}{\dot{\varepsilon}R} = -\frac{\sigma}{2dR(t)/dt}. \tag{5}$$

The EC regime is characterized by a constant extensional rate, and for each concentration, the rate is distinct and set by a local balance of forces. The total accumulated strain in the liquid neck, or Hencky strain, $\varepsilon = 2\ln(R_0/R(t))$, continuously increases in both EC and TVEC regimes. Following standard protocols in capillary breakup studies,[33,63,75] we show a comparison of the transient extensional viscosity as a function of the Hencky strain in Fig. 7 for no salt and salt added NaCMC solutions. The extensional viscosity response seems qualitatively similar in both cases: strain hardening is observed and the viscoelastic stress seems to saturate, yielding a strain-independent regime, which leads to the measurement of steady, terminal extensional viscosity.

Filament lifespan and apparent universality in radius evolution profile

The filament lifespan, t_f, obtained from the radius evolution data using Anna–McKinley fits is contrasted with the apparent filament span, t_{fa}, obtained by visually examining the radius evolution plot in Fig. 8. The slight mismatch between the values is somewhat expected as even though the Anna–McKinley fit captures the combined effect of elastocapillary and finite extensibility regimes, it is not an exact solution to the force balance. As the radius

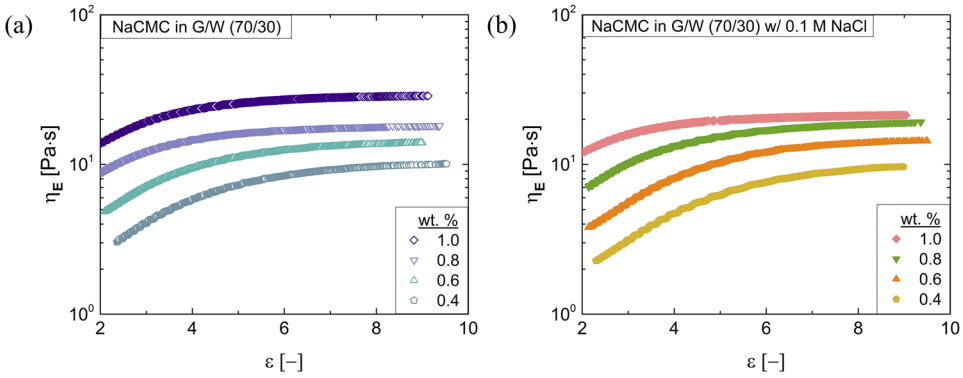

FIG. 7. Extensional rheology response of NaCMC solutions in glycerol/water mixtures. Extensional viscosity as a function of the Hencky strain: (a) no salt system and (b) high salt system. The viscosity plots for all concentrations show strain hardening, as well as the finite extensibility regime that can be analyzed to obtain the steady, terminal extensional viscosity (see Table I).

Published under license by AIP Publishing

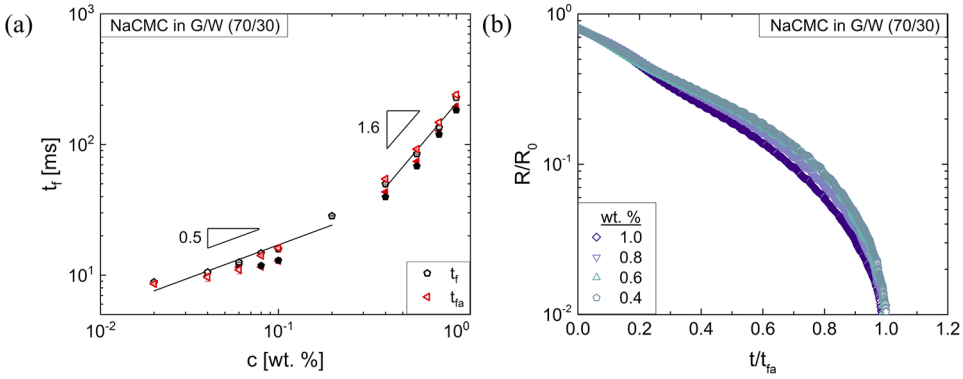

FIG. 8. (a) Filament lifespan as a function of concentration. Two sets of values are obtained: one determined by directly reading the end-point from the datasets and the other from the Anna–McKinley fit. The difference between the two is marginal. (b) Radius evolution profiles plotted against time scaled by the apparent filament span, t_{fa}, show qualitatively similar profiles for entangled solutions.

evolution profiles appear to be quite similar, and partially inspired by the rescaled radius evolution plots for guar gum solutions shown by Torres *et al.*,[18] we plot the radius evolution data as a function of scaled time, by taking the ratio of time to the filament lifespan. The qualitative shape of the curves appears to be matched, but the apparent universal curve requires knowledge of how filament lifespan itself depends on the concentration [see Table I and Fig. 8(a)]. The concentration-dependent increase shows a power law dependence of $c^{1.6}$ that cannot be anticipated by the scaling observed in the steady shear viscosity datasets shown in Figs. 3 and 4.

Extensional relaxation time and steady, terminal extensional viscosity

The terminal extensional viscosity values as a function of concentration are shown in Fig. 9(a) and included in Table I. In the semi-dilute, unentangled regime, $\eta_E^\infty \propto \lambda_E$ or terminal extensional viscosity values are nearly proportional to the extensional relaxation time. The corresponding concentration dependence in the entangled regime is nearly linear in concentration for terminal extensional viscosity, $\eta_E^\infty \propto c^{1.1}$; however, the extensional relaxation time displays a stronger dependence, $\lambda_E \propto c^{1.7}$. Recently, Dinic and Sharma[53] reexamined the relationship between λ_E and η_E^∞ to argue that the linear relationship $\eta_E^\infty \propto \lambda_E$ observed first by Stelter *et al.*[61,62] for both flexible and semi-flexible polymers was a consequence of making the comparisons in the semi-dilute, unentangled regime for a restricted concentration range ($1 < c/c^* < 3$). The experimental results for NaCMC solutions show that a breakdown in linear dependence could occur in entangled systems or if an expanded concentration range is considered.

The ratio of the steady, terminal extensional viscosity and the corresponding zero shear viscosity values can be used for estimating the terminal Trouton ratio as $Tr^\infty = \eta_{E\infty}/\eta_0$. In the unentangled regime, values increase with concentration in range from $Tr^\infty = 20$ to 30 for no added salt, whereas the salt added solutions show significantly higher values in the range of $Tr^\infty = \eta_{E\infty}/\eta_0 = 90$–$120$. In entangled solutions, the values of Tr^∞ show a concentration-dependent decline, and at 1 wt. %, $Tr^\infty = 16$ is obtained both with and without salt. However, as entangled solutions exhibit substantial shear thinning, the apparent Trouton ratios at matched deformation rates are expected to be higher. Dinic *et al.* showed[50] that the absolute values of the extensional viscosity of intrinsically semi-dilute, unentangled polymer solutions (PEO, $M_w = 10^6$ Da) are 250–3200 times higher than their zero shear viscosity, and in dilute PEO solutions, $Tr^\infty = 10^3$–10^6 can be observed. The value of the terminal Trouton ratio depends on both the absolute value of zero shear viscosity and extensional viscosity, which depends on extensibility, $L = R_{\max}/\langle R^2\rangle^{1/2} = N_K^{1-\upsilon}$ (defined as the ratio of the size of a chain stretched by flow to the size of the unperturbed coil). As extensibility depends both on the value of the solvent quality exponent υ and the

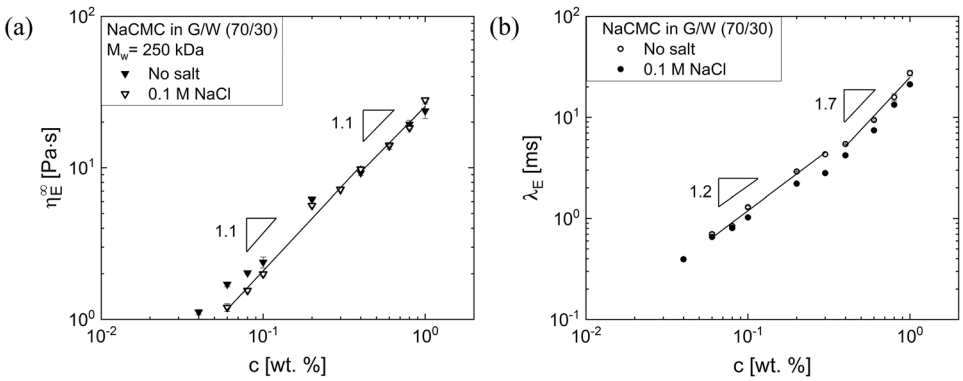

FIG. 9. (a) Terminal, steady extensional viscosity and (b) extensional relaxation time both show similar concentration-dependent variation in the semi-dilute, unentangled regime for no added salt (open symbols) and high salt (closed symbols) solutions. However, in the entangled regime, the concentration-dependent increase in relaxation time shows a larger exponent ($\lambda_E \propto c^{1.7}$) than displayed by terminal extensional viscosity, $\eta_E^\infty \propto c^{1.1}$.

Published under license by AIP Publishing

number of Kuhn segments, N_K (or molecular weight), neutral polymers such as PEO are more extensible than polysaccharides and polyelectrolytes of similar molecular weight and, hence, have a higher Tr^{∞} value. Likewise, higher Tr^{∞} for excess salt NaCMC solutions is due to higher extensibility, correlated with a decrease in coil size on addition of salt, even though R_{max} remains unaffected.

Extensional relaxation time λ_E values obtained from the elastocapillary response are shown in Fig. 9(b) for both no salt and excess salt solutions. The addition of salt causes a minimal decrease in the extensional relaxation time, but the values are nearly identical. In contrast, the specific viscosity values show a significant difference in absolute values at matched concentration and exhibit a distinct concentration-dependent variation in the unentangled regime. The NaCMC solutions in the glycerol-water mixture (70/30 w/w) show a concentration-dependent scaling of $\lambda_E \propto c^{1.2}$ in the semi-dilute, unentangled regime and $\lambda_E \propto c^{1.7}$ in the semi-dilute, entangled regime. The scaling exponent for concentration dependence in the entangled regime is similar to the exponent observed for filament lifespan, but the exponents obtained for filament lifespan in the unentangled regime are somewhat lower. The concentration-dependent scaling behavior shown by λ_E data in both regimes is strikingly different from the shear relaxation time values predicted by scaling theory to be $\lambda \propto c^{-1/2}$, in the semi-dilute, unentangled and the entangled regime, $\lambda \propto c^0$ (independent of concentration), respectively, and measured experimentally. In contrast, in a previous contribution,[52] we found that the data acquired using DoS rheometry for poly(acrylic acid) or PAA solutions exhibit a concentration-dependent scaling of $\lambda_E \propto c^{1/2}$ for the unentangled, semi-dilute regime and $\lambda_E \propto c^{3/2}$ for the entangled regime. The observed concentration-dependent increase in extensional relaxation time for NaCMC solutions (as well as those reported for PAA) is much weaker than $\lambda_E \propto c^{14/3}$ reported for the aqueous solutions of a neutral polymer, polyethylene oxide (PEO) in the entangled regime using CaBER measurements[127,128] and $\lambda_E \propto c^{3.8}$ reported for entangled solutions of cellulose in an ionic liquid.[129]

Since the measured values of extensional relaxation time (ranging from 0.4 ms to 27 ms) listed in Table I are relatively short, the role of viscoelasticity is apparent only at high deformation rates, which are spontaneously generated in thinning liquid necks, and can also be realized in high speed coating, extrusion, and flow through porous media. The experimental results for the overall pinch-off time, as well as the measured relaxation times of the semi-dilute polyelectrolyte solutions, also show that the effect of the increase in solvent viscosity on addition of glycerol is offset to some extent by a decrease in the pervaded volume of the polyelectrolyte chains. However, even though addition of salt leads to a difference in overlap concentration, intrinsic viscosity, pervaded volume, c_e/c^*, and measured specific viscosity values, the extensional relaxation time and terminal extensional viscosity hardly change on addition of salt as the stretched chains in the presence and absence of salt are hydrodynamically equivalent in semi-dilute solutions made in the glycerol-water mixture.

The NaCMC solutions show a relatively short elastocapillary region, in contrast to the well-defined transition from the IC to EC regime observed for experiments carried out with more flexible polymers,[49–53,65,130,131] including neutral polymers such as PEO (M_w = 300 kDa, 600 kDa, 1000 kDa, 2000 kDa, and 5000 kDa) and charged polymers such as PAA solutions (M_w = 450 kDa). In fact, the λ_E values are measurable for $c > 0.05c^*$ for aqueous PEO solutions, and as the prolonged elastocapillary regime leads to a significant delay in pinch-off, the EC contribution dictates the overall filament lifespan.[53] In contrast, even the semi-dilute, unentangled solutions of NaCMC in the glycerol-water mixture pinch-off in relatively short time and emulate the behavior shown by NaPSS solutions:[52] in both cases, the pronounced electrostatics-induced stretching and lower extensibility are at play, whereas for more flexible polymers, the onset and span of the elastocapillary regime are presumably set by coil-stretch transition and hysteresis.[52,53,124]

Cellulose gum as food thickener

The addition of NaCMC increases shear and extensional viscosity of both aqueous and glycerol-added solutions substantially. Practically, for the same weight fraction, polyelectrolytes such as NaCMC boost shear viscosity more significantly than neutral polymers or gums of comparable molecular weight. Decreasing the amount of rheological modifier needed for comparable shear viscosity enhancement leads to lower material costs. Stretching due to electrostatic interactions leads to more expanded conformations for polyelectrolytes, leading to a significantly lower overlap concentration in contrast to neutral polymers. However, the concentration-dependent viscosity increase and the coil size as well as overlap concentration are all quite sensitive to addition of salt as well as glycerol, both of which tend to be ingredients in many food products. In particular, we found that the addition of glycerol leads to a decrease in intrinsic viscosity and, thus, a decrease in pervaded coil size that to some extent off-sets the thickening effect expected on the basis of an increase in solvent viscosity. Addition of salt exercises a much stronger influence on electrostatic interactions and the shear rheology response.

The DoS rheometry protocols emulate the heuristic tests of thickening, stickiness, or cohesiveness based on dripping a sauce from a ladle or practically emulate dispensing of a controlled volume of a fluid. As inviscid, viscous, power law and viscoelastic fluids exhibit distinct neck shape before pinch-off, a qualitative difference in formulation rheology can be obtained by just examining snapshots obtained using the DoS rheometry setup. The quantitative analysis of the neck thinning dynamics yields extensional rheology response, and the solutions that display shear thinning are strain hardening in response to extensional flow fields. The steady, terminal extensional viscosity and extensional relaxation time of NaCMC solutions in the glycerol/water mixture were found to be insensitive to the amount of salt added, even though the zero shear viscosity significantly decreased on salt addition. The addition of NaCMC at $c < 1$ wt. % exercises a profound influence on zero shear viscosity or rate-dependent shear viscosity, and yet, the low extensibility of charged polysaccharides results in a relatively short elastocapillary regime. The combination of suitable shear thinning behavior and relatively short filament lifespan (and suppression of satellite drop formation) are ideal for drop formation and liquid transfer applications. However, longer breakup times are desirable for promoting cohesiveness, stringiness, or stickiness. Extensional viscosity, filament lifespan, and perceived stringiness or stickiness of formulations all increase progressively with polymer concentration (and molecular weight). We envision that DoS rheometry protocols

Published under license by AIP Publishing

will be used in both qualitative and quantitative characterization of recipes for sauces or diets for dysphagia management. Additionally, we hope that the understanding of how both shear rheology and extensional rheology of charged polysaccharide cellulose gum are influenced by the addition of glycerol and salt will provide ability for designing food formulations with tunable flow properties.

CONCLUSIONS

We characterized the shear and extensional rheology response of solutions of sodium carboxymethyl cellulose (NaCMC) or cellulose gum (M_w = 250 kDa), a polysaccharide with charge-bearing repeating groups often used as a rheology modifier in food formulations. NaCMC in aqueous solutions exhibit a remarkably low value of overlap concentration, c^* = 0.007 wt. % (neutral, flexible polymer PEO of M_w = 1000 kDa shows c^* = 0.17 wt. %),[50,53] which increases upon addition of glycerol (in 70/30 w/w mixture) to c^* = 0.03 wt. % and rises further to c^* = 0.06 wt. % upon addition of just 0.005M salt and to c^* = 0.12 wt. % upon addition of 0.1M salt to the mixed solvent. The addition of salt leads to a substantial drop in specific viscosity. Additionally, even though glycerol, a higher viscosity miscible solvent, is often added to increase the solution viscosity, our results show that a decrease in the pervaded volume of charged macromolecules significantly offsets the impact of higher solvent viscosity. The concentration-dependent increase in the specific viscosity exhibits $\eta_{sp} \propto c^{0.62}$ and $\eta_{sp} \propto c^{3/2}$ for aqueous NaCMC solutions, close to values anticipated by scaling theory. In contrast, the solutions in the glycerol-water mixture (70/30 w/w) show a stronger concentration dependence of $\eta_{sp} \propto c^{0.95}$ and $\eta_{sp} \propto c^{2.8}$, respectively, for no added salt, and $\eta_{sp} \propto c^{1.6}$ and $\eta_{sp} \propto c^{2.8}$ on addition of salt. The entanglement concentration c_e = 0.37 wt. % for aqueous solution is comparable to c_e = 0.5 wt. % for solutions in the glycerol-water mixture, but as c^* increases on addition of glycerol, the value c_e/c^* = 53 decreases to c_e/c^* = 17. In addition to electrostatics, changes in effective solvent quality, hydrophobic effect, and hydrogen bonding contribute to stronger exponents for NaCMC solutions in glycerol-water mixtures and influence the observed value of c^* and c_e/c^*.

We characterized the pinch-off dynamics and extensional rheology response of NaCMC solutions in the glycerol-water mixture (70/30 w/w) using dripping-onto-substrate (DoS) rheometry protocols. Due to the electrostatic pre-stretching of chains, NaCMC chains exist in a relatively extended conformation and, due to longer persistence length and fewer Kuhn segments, the elastocapillary regime for all NaCMC solutions appears to have a much shorter span than observed for flexible neutral polymers such as PEO. In the semi-dilute unentangled regime, the measured values of both η_E^∞ and λ_E appear to show a nearly matched linear concentration dependence for NaCMC solutions in the glycerol-water mixture. However, in the entangled regime, η_E^∞ exhibits a nearly linear increase in contrast to a stronger power law observed for extensional relaxation time, $\lambda_E \sim c^{1.7}$. Most importantly, the addition of salt has relatively little influence on the magnitude or a concentration-dependent increase in η_E^∞ and λ_E of NaCMC solutions, even though the shear rheology response is markedly distinct. Finally, the Trouton ratio, $Tr^\infty = \eta_{E\infty}/\eta_0$, determined from rate-independent extensional and shear viscosity values increases Tr^∞ = 20–30 for no added salt in semi-dilute, unentangled solutions. Significantly higher values $Tr^\infty = \eta_{E\infty}/\eta_0$ = 90–120 are obtained in high salt (0.1M) solutions in the glycerol-water mixture (70/30 in w/w). However, in entangled solutions, the values of Tr^∞ show a concentration-dependent decline, and at 1%, Tr^∞ = 16 is obtained both with and without salt. Thus, NaCMC (M_w = 250 kg/mol) as a food thickener provides a substantial increase in zero shear viscosity and adequate degree of shear thinning but without substantially changing capillary breakup and dispensing behavior. We envision and hope that the DoS rheometry protocols described herein will inspire food scientists and engineers to investigate the extensional rheology response and design food products with a better understanding of the complex interplay between electrostatics and macromolecular hydrodynamics, as well as a better (quantitative, rather than heuristic) understanding of the response to extensional flows in culinary applications.

SUPPLEMENTARY MATERIAL

See the supplementary material for four videos showing capillary-driven thinning and breakup of NaCMC solutions that are included online and for a table that lists the exponents and errors obtained by fitting the concentration-dependent values reported in this manuscript.

ACKNOWLEDGMENTS

V.S. would like to acknowledge partial funding support from the 3M Non-Tenured Faculty Award. The students (L.N.J. and C.D.V.M.N.) wish to acknowledge sustained funding (Teaching Assistantship) by the Department of Chemistry at UIC. V.S. would like to thank Professor Samanvaya Srivasatava, UCLA, and Professor Amanda Marciel, Rice, for a close reading of the manuscript. V.S. also wishes to acknowledge Professor Peter Fischer and Professor Erich Windhab for inviting him to the 8th International Symposium on Food Rheology and Structure–ISFRS 2019 in ETH, Zurich, and providing a motivation for this study.

REFERENCES

[1] T. Wüstenberg, *Cellulose and Cellulose Derivatives in the Food Industry: Fundamentals and Applications* (John Wiley & Sons, 2014).
[2] E. Dickinson, "Hydrocolloids as emulsifiers and emulsion stabilizers," Food Hydrocolloids **23**, 1473 (2009).
[3] P. Fischer and E. J. Windhab, "Rheology of food materials," Curr. Opin. Colloid Interface Sci. **16**, 36 (2011).
[4] R. Lapasin and S. Pricl, *Rheology of Industrial Polysaccharides: Theory and Applications* (Chapman & Hall, London, 1995).
[5] S. Dumitriu, *Polysaccharides: Structural Diversity and Functional Versality* (Marcel Dekker, New York, 2005).
[6] C. Clasen and W. M. Kulicke, "Determination of viscoelastic and rheo-optical material functions of water-soluble cellulose derivatives," Prog. Polym. Sci. **26**, 1839 (2001).
[7] R. Lambourne and T. A. Striven, *Paint and Surface Coatings: Theory and Practice* (Woodhead Publishing Ltd., Cambridge, UK, 1999).
[8] S. Morozova, P. W. Schmidt, A. Metaxas, F. S. Bates, T. P. Lodge, and C. S. Dutcher, "Extensional flow behavior of methylcellulose solutions containing fibrils," ACS Macro Lett. **7**, 347 (2018).
[9] G. Savary, M. Grisel, and C. Picard, "Cosmetics and personal care products," in *Natural Polymers: Industry Techniques and Applications*, edited by O. Olatunji (Springer, 2016).

Published under license by AIP Publishing

[10]K. M. N. Oates, W. E. Krause, R. L. Jones, and R. H. Colby, "Rheopexy of synovial fluid and protein aggregation," J. R. Soc., Interface **3**, 167 (2006).
[11]S. J. Haward, V. Sharma, and J. A. Odell, "Extensional opto-rheometry with biofluids and ultra-dilute polymer solutions," Soft Matter **7**, 9908 (2011).
[12]E. Puchelle, J. Zahm, and C. Duvivier, "Spinability of bronchial mucus. Relationship with viscoelasticity and mucous transport properties," Biorheology **20**, 239 (1983).
[13]P. Erni, M. Varagnat, C. Clasen, J. Crest, and G. H. McKinley, "Microrheometry of sub-nanolitre biopolymer samples: non-Newtonian flow phenomena of carnivorous plant mucilage," Soft Matter **7**, 10889 (2011).
[14]L. Gaume and Y. Forterre, "A viscoelastic deadly fluid in carnivorous pitcher plants," PLoS One **2**, e1185 (2007).
[15]C. Arancibia, S. Bayarri, and E. Costell, "Comparing carboxymethyl cellulose and starch as thickeners in oil/water emulsions. Implications on rheological and structural properties," Food Biophys. **8**, 122 (2013).
[16]M. Bahramparvar and M. Mazaheri Tehrani, "Application and functions of stabilizers in ice cream," Food Rev. Int. **27**, 389 (2011).
[17]M. A. Cancela, E. Alvarez, and R. Maceiras, "Effects of temperature and concentration on carboxymethylcellulose with sucrose rheology," J. Food Eng. **71**, 419 (2005).
[18]M. D. Torres, B. Hallmark, and D. I. Wilson, "Effect of concentration on shear and extensional rheology of guar gum solutions," Food Hydrocolloids **40**, 85 (2014).
[19]M. D. Torres, B. Hallmark, D. I. Wilson, and L. Hilliou, "Natural giesekus fluids: Shear and extensional behavior of food gum solutions in the semidilute regime," AIChE J. **60**, 3902 (2014).
[20]M. T. Ghannam and M. N. Esmail, "Rheological properties of carboxymethyl cellulose," J. Appl. Polym. Sci. **64**, 289 (1997).
[21]F. A. Ismail, E. T. El-Ashwah, and S. A. El-Farra, "The practical aspects of viscosity of carboxymethylcellulose in dietetic foods," J. Consum. Stud. Home Econ. **4**, 269 (1980).
[22]E. Malinauskytė, J. Ramanauskaitė, D. Leskauskaitė, T. G. Devold, R. B. Schüller, and G. E. Vegarud, "Effect of human and simulated gastric juices on the digestion of whey proteins and carboxymethylcellulose-stabilised O/W emulsions," Food Chem. **165**, 104 (2014).
[23]O. Yuliarti, K. H. Mei, Z. K. X. Ting, and K. Y. Yi, "Influence of combination carboxymethylcellulose and pectin on the stability of acidified milk drinks," Food Hydrocolloids **89**, 216 (2019).
[24]R. G. M. Van der Sman, "Soft matter approaches to food structuring," Adv. Colloid Interface Sci. **176**, 18 (2012).
[25]R. Mezzenga, P. Schurtenberger, A. Burbidge, and M. Michel, "Understanding foods as soft materials," Nat. Mater. **4**, 729 (2005).
[26]P. Fischer, M. Pollard, P. Erni, I. Marti, and S. Padar, "Rheological approaches to food systems," C. R. Phys. **10**, 740 (2009).
[27]T. Funami, "*In vivo* and rheological approaches for characterizing food oral processing and usefulness of polysaccharides as texture modifiers-A review," Food Hydrocolloids **68**, 2 (2017).
[28]J.-M. Li and S.-P. Nie, "The functional and nutritional aspects of hydrocolloids in foods," Food Hydrocolloids **53**, 46 (2016).
[29]H. Choi, J. R. Mitchell, S. R. Gaddipati, S. E. Hill, and B. Wolf, "Shear rheology and filament stretching behaviour of xanthan gum and carboxymethyl cellulose solution in presence of saliva," Food Hydrocolloids **40**, 71 (2014).
[30]K. Nishinari, M. Turcanu, M. Nakauma, and Y. Fang, "Role of fluid cohesiveness in safe swallowing," npj Sci. Food **3**, 5 (2019).
[31]J. L. Kokini and K. Surmay, "Steady shear viscosity, first normal stress difference and recoverable strain in carboxymethyl cellulose, sodium alginate and guar gum," Carbohydr. Polym. **23**, 27 (1994).
[32]C. J. S. Petrie, "One hundred years of extensional flow," J. Non-Newtonian Fluid Mech. **137**, 1 (2006).
[33]G. H. McKinley, "Visco-elasto-capillary thinning and break-up of complex fluids," Rheol. Rev. **1**, 1–38 (2005).
[34]G. H. McKinley and T. Sridhar, "Filament-stretching rheometry of complex fluids," Annu. Rev. Fluid Mech. **34**, 375 (2002).
[35]T. Q. Nguyen and H. H. Kausch, *Flexible Polymer Chains in Elongational Flow: Theory and Experiment* (Springer-Verlag, Berlin, 1999).
[36]F. Rodriguez-Gonzalez and L. A. Bello-Perez, "Extensional properties of macromolecules," Curr. Opin. Food Sci. **9**, 98 (2016).
[37]S. Różańska, "Extensional rheology in food processing," in *Advances in Food Rheology and its Applications*, edited by J. Ahmed, P. Ptaszek, and S. Basu (Elsevier, 2017).
[38]J. R. Stokes, M. W. Boehm, and S. K. Baier, "Oral processing, texture and mouthfeel: From rheology to tribology and beyond," Curr. Opin. Colloid Interface Sci. **18**, 349 (2013).
[39]E. Brito-de la Fuente, M. Turcanu, O. Ekberg, and C. Gallegos, "Rheological aspects of swallowing and dysphagia: Shear and elongational flows," in *Dysphagia* (Springer, 2017).
[40]M. Q. Waqas, J. Wiklund, A. Altskär, O. Ekberg, and M. Stading, "Shear and extensional rheology of commercial thickeners used for dysphagia management," J. Texture Stud. **48**, 507 (2017).
[41]T. van Vliet, A. M. Janssen, A. H. Bloksma, and P. Walstra, "Strain hardening of dough as a requirement for gas retention," J. Texture Stud. **23**, 439 (1992).
[42]T. van Vliet, "Strain hardening as an indicator of bread-making performance: A review with discussion," J. Cereal Sci. **48**, 1 (2008).
[43]C. I. Moraru and J. L. Kokini, "Nucleation and expansion during extrusion and microwave heating of cereal foods," Compr. Rev. Food Sci. Food Saf. **2**, 147 (2003).
[44]P. G. de Gennes, "Coil-stretch transition of dilute flexible polymers under ultrahigh velocity gradients," J. Chem. Phys. **60**, 5030 (1974).
[45]R. G. Larson, "The rheology of dilute solutions of flexible polymers: Progress and problems," J. Rheol. **49**, 1 (2005).
[46]C. M. Schroeder, H. P. Babcock, E. S. G. Shaqfeh, and S. Chu, "Observation of polymer conformation hysteresis in extensional flow," Science **301**, 1515 (2003).
[47]C. M. Schroeder, "Single polymer dynamics for molecular rheology," J. Rheol. **62**, 371 (2018).
[48]D. F. James and K. Walters, "A critical appraisal of available methods for the measurement of extensional properties of mobile systems," in *Techniques of Rheological Measurement*, edited by A. A. Collyer (Elsevier, New York, 1994).
[49]J. Dinic, Y. Zhang, L. N. Jimenez, and V. Sharma, "Extensional relaxation times of dilute, aqueous polymer solutions," ACS Macro Lett. **4**, 804 (2015).
[50]J. Dinic, M. Biagioli, and V. Sharma, "Pinch-off dynamics and extensional relaxation times of intrinsically semi-dilute polymer solutions characterized by dripping-onto-substrate rheometry," J. Polym. Sci., Part B: Polym. Phys. **55**, 1692 (2017).
[51]J. Dinic, L. N. Jimenez, and V. Sharma, "Pinch-off dynamics and dripping-onto-substrate (DoS) rheometry of complex fluids," Lab Chip **17**, 460 (2017).
[52]L. N. Jimenez, J. Dinic, N. Parsi, and V. Sharma, "Extensional relaxation time, pinch-off dynamics and printability of semi-dilute polyelectrolyte solutions," Macromolecules **51**, 5191 (2018).
[53]J. Dinic and V. Sharma, "Macromolecular relaxation, strain, and extensibility determine elastocapillary thinning and extensional viscosity of polymer solutions," Proc. Natl. Acad. Sci. U. S. A. **116**, 8766 (2019).
[54]K. A. Marshall, A. M. Liedtke, A. H. Todt, and T. W. Walker, "Extensional rheometry with a handheld mobile device," Exp. Fluids **58-69**, 9 (2017).
[55]J. Eggers and M. A. Fontelos, *Singularities: Formation, Structure, and Propagation* (Cambridge University Press, Cambridge, UK, 2015).
[56]P. K. Notz, A. U. Chen, and O. A. Basaran, "Satellite drops: Unexpected dynamics and change of scaling during pinch-off," Phys. Fluids **13**, 549 (2001).
[57]J. R. Castrejón-Pita, A. A. Castrejón-Pita, S. S. Thete, K. Sambath, I. M. Hutchings, J. Hinch, J. R. Lister, and O. A. Basaran, "Plethora of transitions during breakup of liquid filaments," Proc. Natl. Acad. Sci. U. S. A. **112**, 4582 (2015).
[58]A. L. Yarin, *Free Liquid Jets and Films: Hydrodynamics and Rheology* (Longman Scientific & Technical, 1993).
[59]A. V. Bazilevsky, V. M. Entov, and A. N. Rozhkov, *Liquid Filament Microrheometer and Some of its Applications* (Elsevier, Edinburgh, UK, 1990).
[60]A. V. Bazilevsky, V. M. Entov, and A. N. Rozhkov, "Breakup of a liquid bridge as a method of rheological testing of biological fluids," Fluid Dyn. **46**, 613 (2011).
[61]M. Stelter, G. Brenn, A. L. Yarin, R. P. Singh, and F. Durst, "Validation and application of a novel elongational device for polymer solutions," J. Rheol. **44**, 595 (2000).

Published under license by AIP Publishing

[62]M. Stelter, G. Brenn, A. L. Yarin, R. P. Singh, and F. Durst, "Investigation of the elongational behavior of polymer solutions by means of an elongational rheometer," J. Rheol. **46**, 507 (2002).
[63]S. L. Anna and G. H. McKinley, "Elasto-capillary thinning and breakup of model elastic liquids," J. Rheol. **45**, 115 (2001).
[64]L. E. Rodd, T. P. Scott, J. J. Cooper-White, and G. H. McKinley, "Capillary break-up rheometry of low-viscosity elastic fluids," Appl. Rheol. **15**, 12 (2005).
[65]V. Tirtaatmadja, G. H. McKinley, and J. J. Cooper-White, "Drop formation and breakup of low viscosity elastic fluids: Effects of molecular weight and concentration," Phys. Fluids **18**, 043101 (2006).
[66]P. P. Bhat, S. Appathurai, M. T. Harris, M. Pasquali, G. H. McKinley, and O. A. Basaran, "Formation of beads-on-a-string structures during break-up of viscoelastic filaments," Nat. Phys. **6**, 625 (2010).
[67]T. Wunderlich, M. Stelter, T. Tripathy, B. R. Nayak, G. Brenn, A. L. Yarin, R. P. Singh, P. O. Brunn, and F. Durst, "Shear and extensional rheological investigations in solutions of grafted and ungrafted polysaccharides," J. Appl. Polym. Sci. **77**, 3200 (2000).
[68]M. R. Duxenneuner, P. Fischer, E. J. Windhab, and J. J. Cooper-White, "Extensional properties of hydroxypropyl ether guar gum solutions," Biomacromolecules **9**, 2989 (2008).
[69]J. P. Plog, W. M. Kulicke, and C. Clasen, "Influence of the molar mass distribution on the elongational behaviour of polymer solutions in capillary breakup," Appl. Rheol. **15**, 28 (2005).
[70]D. Szopinski, U. A. Handge, W.-M. Kulicke, V. Abetz, and G. A. Luinstra, "Extensional flow behavior of aqueous guar gum derivative solutions by capillary breakup elongational rheometry (CaBER)," Carbohydr. Polym. **136**, 834 (2016).
[71]A. Ö. Bingöl, D. Lohmann, K. Püschel, and W.-M. Kulicke, "Characterization and comparison of shear and extensional flow of sodium hyaluronate and human synovial fluid," Biorheology **47**, 205 (2010).
[72]H. Storz, U. Zimmermann, H. Zimmermann, and W.-M. Kulicke, "Viscoelastic properties of ultra-high viscosity alginates," Rheol. Acta **49**, 155 (2010).
[73]R. De Dier, W. Mathues, and C. Clasen, "Extensional flow and relaxation of semi-dilute solutions of schizophyllan," Macromol. Mater. Eng. **298**, 944 (2013).
[74]C. Rodríguez-Rivero, L. Hilliou, E. M. M. del Valle, and M. A. Galán, "Rheological characterization of commercial highly viscous alginate solutions in shear and extensional flows," Rheol. Acta **53**, 559 (2014).
[75]L. Campo-Deano and C. Clasen, "The slow retraction method (SRM) for the determination of ultra-short relaxation times in capillary breakup extensional rheometry experiments," J. Non-Newtonian Fluid Mech. **165**, 1688 (2010).
[76]E. Miller, C. Clasen, and J. P. Rothstein, "The effect of step-stretch parameters on capillary breakup extensional rheology (CaBER) measurements," Rheol. Acta **48**, 625 (2009).
[77]S. S. Vadodaria and R. J. English, "Extensional rheometry of cellulose ether solutions: Flow instability," Cellulose **23**, 339 (2016).
[78]EFSA ANS Panel, A. Mortensen, F. Aguilar, R. Crebelli, A. Di Domenico, B. Dusemund, M. J. Frutos, P. Galtier, D. Gott, U. Gundert-Remy *et al.*, "Re-evaluation of glycerol (E 422) as a food additive," EFSA J. **15**, e04720 (2017).
[79]C. G. Lopez, R. H. Colby, and J. T. Cabral, "Electrostatic and hydrophobic interactions in NaCMC aqueous solutions: Effect of degree of substitution," Macromolecules **51**, 3165 (2018).
[80]C. G. Lopez, R. H. Colby, P. Graham, and J. T. Cabral, "Viscosity and scaling of semiflexible polyelectrolyte NaCMC in aqueous salt solutions," Macromolecules **50**, 332 (2017).
[81]C. G. Lopez, S. E. Rogers, R. H. Colby, P. Graham, and J. T. Cabral, "Structure of sodium carboxymethyl cellulose aqueous solutions: A SANS and rheology study," J. Polym. Sci., Part B: Polym. Phys. **53**, 492 (2015).
[82]X. H. Yang and W. L. Zhu, "Viscosity properties of sodium carboxymethylcellulose solutions," Cellulose **14**, 409 (2007).
[83]D. Charpentier-Valenza, L. Merle, G. Mocanu, L. Picton, and G. Muller, "Rheological properties of hydrophobically modified carboxymethylcelluloses," Carbohydr. Polym. **60**, 87 (2005).
[84]S. Dapía, C. A. Tovar, V. Santos, and J. C. Parajó, "Rheological behaviour of carboxymethylcellulose manufactured from TCF-bleached milox pulps," Food Hydrocolloids **19**, 313 (2005).
[85]E. H. DeButts, J. A. Hudy, and J. H. Elliott, "Rheology of sodium carboxymethylcellulose solutions," Ind. Eng. Chem. **49**, 94 (1957).
[86]J. H. Elliot and A. J. Ganz, "Some rheological properties of sodium carboxymethylcellulose solutions and gels," Rheol. Acta **13**, 670 (1974).
[87]J. Horinaka, K. Chen, and T. Takigawa, "Entanglement properties of carboxymethyl cellulose and related polysaccharides," Rheol. Acta **57**, 51 (2018).
[88]P. Komorowska, S. Różańska, and J. Różański, "Effect of the degree of substitution on the rheology of sodium carboxymethylcellulose solutions in propylene glycol/water mixtures," Cellulose **24**, 4151 (2017).
[89]C. G. Lopez and W. Richtering, "Influence of divalent counterions on the solution rheology and supramolecular aggregation of carboxymethyl cellulose," Cellulose **26**, 1517 (2019).
[90]K. W. Hsiao, J. Dinic, Y. Ren, V. Sharma, and C. M. Schroeder, "Passive non-linear microrheology for determining extensional viscosity," Phys. Fluids **29**, 121603 (2017).
[91]A. V. Walter, L. N. Jimenez, J. Dinic, V. Sharma, and K. A. Erk, "Effect of salt valency and concentration on shear and extensional rheology of aqueous polyelectrolyte solutions for enhanced oil recovery," Rheol. Acta **58**, 145 (2019).
[92]N. S. Suteria, S. Gupta, R. Potineni, S. K. Baier, and S. A. Vanapalli, "eCapillary: a disposable microfluidic extensional viscometer for weakly elastic polymeric fluids," Rheol. Acta **58**, 403 (2019).
[93]K. A. Marshall and T. W. Walker, "Investigating the dynamics of droplet breakup in a microfluidic cross-slot device for characterizing the extensional properties of weakly-viscoelastic fluids," Rheol. Acta **58**, 573 (2019).
[94]M. Rosello, S. Sur, B. Barbet, and J. P. Rothstein, "Dripping-onto-substrate capillary breakup extensional rheometry of low-viscosity printing inks," J. Non-Newtonian Fluid Mech. **266**, 160 (2019).
[95]Y. Zhang and S. J. Muller, "Unsteady sedimentation of a sphere in wormlike micellar fluids," Phys. Rev. Fluids **3**, 043301 (2018).
[96]S. J. Wu and H. Mohammadigoushki, "Sphere sedimentation in wormlike micelles: Effect of micellar relaxation spectrum and gradients in micellar extensions," J. Rheol. **62**, 1061 (2018).
[97]R. Omidvar, S. Wu, and H. Mohammadigoushki, "Detecting wormlike micellar microstructure using extensional rheology," J. Rheol. **63**, 33 (2019).
[98]V. Sharma, S. J. Haward, J. Serdy, B. Keshavarz, A. Soderlund, P. Threlfall-Holmes, and G. H. McKinley, "The rheology of aqueous solutions of ethyl hydroxy-ethyl cellulose (EHEC) and its hydrophobically modified analogue (hmEHEC): Extensional flow response in capillary break-up, jetting (ROJER) and in a cross-slot extensional rheometer," Soft Matter **11**, 3251 (2015).
[99]A. V. Dobrynin, "Solutions of charged polymers," Polym. Sci.: Compr. Ref. **1**, 81 (2012).
[100]A. V. Dobrynin, R. H. Colby, and M. Rubinstein, "Scaling theory of polyelectrolyte solutions," Macromolecules **28**, 1859 (1995).
[101]A. V. Dobrynin and M. Rubinstein, "Theory of polyelectrolytes in solutions and at surfaces," Prog. Polym. Sci. **30**, 1049 (2005).
[102]R. M. Fuoss and U. P. Strauss, "Polyelectrolytes. II. Poly-4-vinylpyridonium chloride and poly-4-vinyl-*N*-*n*-butylpyridonium bromide," J. Polym. Sci. **3**, 246 (1948).
[103]R. M. Fuoss, "Polyelectrolytes," Discuss. Faraday Soc. **11**, 125 (1951).
[104]M. Muthukumar, "A perspective on polyelectrolyte solutions," Macromolecules **50**, 9528 (2017).
[105]M. Muthukumar, "Dynamics of polyelectrolyte solutions," J. Chem. Phys. **107**, 2619 (1997).
[106]R. H. Colby, "Structure and linear viscoelasticity of flexible polymer solutions: Comparison of polyelectrolyte and neutral polymer solutions," Rheol. Acta **49**, 425 (2010).
[107]D. C. Boris and R. H. Colby, "Rheology of sulfonated polystyrene solutions," Macromolecules **31**, 5746 (1998).
[108]S. Dou and R. H. Colby, "Solution rheology of a strongly charged polyelectrolyte in good solvent," Macromolecules **41**, 6505 (2008).
[109]H. Eisenberg and J. Pouyet, "Viscosities of dilute aqueous solutions of a partially quaternized poly-4-vinyl pyridine at low gradients of flow," J. Polym. Sci. **13**, 85 (1954).

Published under license by AIP Publishing

[110]I. Roure, M. Rinaudo, M. Milas, and E. Frollini, "Viscometric behaviour of polyelectrolytes in the presence of low salt concentration," Polymer **39**, 5441 (1998).
[111]C. Holm, J. F. Joanny, K. Kremer, R. R. Netz, P. Reineker, C. Seidel, T. A. Vilgis, and R. G. Winkler, "Polyelectrolyte theory," in *Polyelectrolytes with Defined Molecular Architecture II* (Springer, 2004).
[112]M. Muthukumar, "Polyelectrolyte dynamics," Adv. Chem. Phys. **131**, 1 (2005).
[113]N. B. Wyatt and M. W. Liberatore, "Rheology and viscosity scaling of the polyelectrolyte xanthan gum," J. Appl. Polym. Sci. **114**, 4076 (2009).
[114]W. E. Krause, J. S. Tan, and R. H. Colby, "Semidilute solution rheology of polyelectrolytes with no added salt," J. Polym. Sci., Part B: Polym. Phys. **37**, 3429 (1999).
[115]T. A. Witten and P. Pincus, "Structure and viscosity of interpenetrating polyelectrolyte chains," Europhys. Lett. **3**, 315 (1987).
[116]J. Cohen and Z. Priel, "Viscosity of dilute polyelectrolyte solutions: Temperature dependence," J. Chem. Phys. **93**, 9062 (1990).
[117]S. P. Chen and L. A. Archer, "Relaxation dynamics of salt-free polyelectrolyte solutions using flow birefringence and rheometry," J. Polym. Sci., Part B: Polym. Phys. **37**, 825 (1999).
[118]Y.-J. Chen and P. Steen, "Dynamics of inviscid capillary breakup: Collapse and pinchoff of a film bridge," J. Fluid Mech. **341**, 245 (1997).
[119]R. F. Day, E. J. Hinch, and J. R. Lister, "Self-similar capillary pinchoff of an inviscid fluid," Phys. Rev. Lett. **80**, 704 (1998).
[120]J. Eggers, "Nonlinear dynamics and breakup of free-surface flows," Rev. Mod. Phys. **69**, 865 (1997).
[121]J. Dinic and V. Sharma, "Computational analysis of self-similar capillary-driven thinning and pinch-off dynamics during dripping using the volume-of-fluid method," Phys. Fluids **31**, 021211 (2018).
[122]Lord Rayleigh, "On the capillary phenomenon of jets," Proc. R. Soc. London **29**, 71 (1879).
[123]V. M. Entov and E. J. Hinch, "Effect of a spectrum of relaxation times on the capillary thinning of a filament of elastic liquid," J. Non-Newtonian Fluid Mech. **72**, 31 (1997).
[124]C. Clasen, J. P. Plog, W. M. Kulicke, M. Owens, C. Macosko, L. E. Scriven, M. Verani, and G. H. McKinley, "How dilute are dilute solutions in extensional flows?," J. Rheol. **50**, 849 (2006).
[125]J. Zhou and M. Doi, "Dynamics of viscoelastic filaments based on Onsager principle," Phys. Rev. Fluids **3**, 084004 (2018).
[126]C. Wagner, L. Bourouiba, and G. H. McKinley, "An analytic solution for capillary thinning and breakup of FENE-P fluids," J. Non-Newtonian Fluid Mech. **218**, 53 (2015).
[127]O. Arnolds, H. Buggisch, D. Sachsenheimer, and N. Willenbacher, "Capillary breakup extensional rheometry (CaBER) on semi-dilute and concentrated polyethyleneoxide (PEO) solutions," Rheol. Acta **49**, 1207 (2010).
[128]D. Sachsenheimer, B. Hochstein, and N. Willenbacher, "Experimental study on the capillary thinning of entangled polymer solutions," Rheol. Acta **53**, 725 (2014).
[129]S. J. Haward, V. Sharma, C. P. Butts, G. H. McKinley, and S. S. Rahatekar, "Shear and extensional rheology of cellulose/ionic liquid solutions," Biomacromolecules **13**, 1688 (2012).
[130]C. Wagner, Y. Amarouchene, D. Bonn, and J. Eggers, "Droplet detachment and satellite bead formation in viscoelastic fluids," Phys. Rev. Lett. **95**, 164504 (2005).
[131]Y. Amarouchene, D. Bonn, J. Meunier, and H. Kellay, "Inhibition of the finite-time singularity during droplet fission of a polymeric fluid," Phys. Rev. Lett. **86**, 3558 (2001).

Published under license by AIP Publishing